Inorganica Chimica Acta, 165 (1989) 123–129

Bioinorganic Model Complexes for the Active Site in Manganese Containing Catalases. The Crystal Structures of $[L_2Mn^{II}_2(\mu\text{-}OH)(\mu\text{-}O_2CCH_3)_2](PF_6)\cdot CH_3OH$ and $[L'_2Mn^{III}_2(\mu\text{-}O)(\mu\text{-}O_2CCH_3)_2](I_3)I\cdot H_2O$

URSULA BOSSEK, KARL WIEGHARDT*

Lehrstuhl für Anorganische Chemie I, Ruhr-Universität, D-4630 Bochum (F.R.G.)

BERNHARD NUBER and JOHANNES WEISS

Anorganisch-Chemisches Institut der Universität, D-6900 Heidelberg (F.R.G.)

(Received May 2, 1989; revised June 28, 1989)

Abstract

The crystal structures of $[L_2Mn^{II}_2(\mu\text{-}OH)(\mu\text{-}O_2CCH_3)_2](PF_6)\cdot CH_3OH$ (1) and $[L'_2Mn^{III}_2(\mu\text{-}O)(\mu\text{-}O_2CCH_3)_2](I_3)I\cdot H_2O$ (2) have been determined by X-ray crystallography (L = *N,N',N''*-trimethyl-1,4,7-triazacyclononane, $C_9H_{21}N_3$; L' = 1,4,7-triazacyclononane, $C_6H_{15}N_3$). 1 contains the μ-hydroxo-bis(μ-carboxylato)dimanganese(II) core whereas in 2 the μ-oxo-bis(μ-carboxylato)dimanganese(III) entity has been identified. 1 and 2 serve as model compounds for the active site of the manganese containing catalases isolated from *Lactobacillus plantarum* and *Thermus thermophilus.*

Introduction

In recent years at least three enzymes have been isolated and characterized which contain two manganese(III) ions per subunit. From X-ray diffraction data on the catalase from *Thermus thermophilus* a Mn···Mn separation of ≈3.6 Å has been deduced [1]. Electronic [2] and recent ESR spectra [3] of the catalase isolated from *Lactobacillus plantarum* also indicate the presence of a binuclear manganese containing active site. The electronic spectrum of a ribonucleotide reductase from *Brevibacterium ammoniagenes* is also in accord with a binuclear center [4]. For all three enzymes a μ-oxo-bis(μ-carboxylato)dimanganese(III) entity has been proposed which is corroborated by the synthesis of a number of low molecular weight model complexes [5–8]. In particular, binuclear complexes containing the cyclic tridentate amine capping ligands *N,N',N''*-trimethyl-1,4,7-triazacyclononane (L; $C_9H_{21}N_3$) and 1,4,7-triazacyclononane (L'; $C_6H_{15}N_3$) have been synthesized where the manganese ions are in the oxidation states II,II [9, 10]; III,III [5, 10] and III,IV [9, 10]. Electrochemical studies have shown that the oxidation levels II,III and IV,IV are also accessible [9, 10]. Thus successive one electron oxidation and reduction steps occur in a readily accessible potential range which model the behavior of the biomolecules well.

Although a number of crystal structures of such binuclear complexes at the oxidation level II,III [11], III,III [5–7] and III,IV [9], respectively, have been characterized by X-ray crystallography, this information is missing for the corresponding μ-hydroxo-bis(μ-carboxylato)dimanganese(II) core. In a previous communication we reported the structure of $[L'_2Mn^{III}_2(O)(CH_3CO_2)_2](ClO_4)_2$ [5] which was of poor quality due to disorder of the ClO_4^- anions.

Here we wish to report the crystal structures of $[L_2Mn^{II}_2(\mu\text{-}OH)(\mu\text{-}O_2CCH_3)_2](PF_6)\cdot CH_3OH$ (1) and $[L'_2Mn^{III}_2(\mu\text{-}O)(\mu\text{-}O_2CCCH_3)_2](I_3)I\cdot H_2O$ (2).

Experimental

Syntheses

The ligands *N,N',N''*-trimethyl-1,4,7-triazacyclononane (L) and 1,4,7-triazacyclononane (L') were prepared as described in the literature [12, 13].

$[L_2Mn^{II}_2(\mu\text{-}OH)(\mu\text{-}O_2CCH_3)_2](PF_6)\cdot CH_3OH$ *(1)*

To an argon scrubbed solution of L (0.50 g) in methanol (25 ml) was added $Mn(CH_3CO_2)_2\cdot 4H_2O$ (0.30 g) and after 15 min of stirring sodium acetate (0.15 g) was added. This solution was stirred for 15 min at room temperature. After addition of $NaPF_6$ (0.20 g) the solution was allowed to stand at 0 °C for 2 days. Pale-green crystals of 1 of X-ray quality precipitated which were collected by filtration and stored under an argon atmosphere (yield 0.28 g). The preparation of the perchlorate salt of 1 has been described previously [10].

---

*Author to whom correspondence should be addressed.

0020-1693/89/$3.50

$[L'_2Mn^{III}_2(\mu\text{-}O)(\mu\text{-}O_2CCH_3)_3](I_3)I\cdot H_2O$ (2)

The method described here was employed only in order to obtain single crystals suitable for X-ray crystallography. A general good yield synthesis of the perchlorate salt is given in ref. 5.

To a solution of L′ (0.20 g) in methanol (40 ml) was added $Mn(O_2CCH_3)_3\cdot 2H_2O$. After 15 min of stirring at room temperature sodium iodide (0.50 g) was added. A purple precipitate formed within 24 h at room temperature which was filtered off and discarded. Upon standing of the filtrate for further 24 h brown–red crystals of 2 formed (yield 0.40 g). These crystals were suitable for an X-ray structure analysis.

X-ray Crystallography

A quasi-octahedral crystal of **1** and a tabular-shaped red–brown crystal of **2** were attached to a glass fiber and mounted on Syntex R3 and AED II (Siemens) diffractometers, respectively. The unit cell dimensions, details of intensity measurements and data reduction are summarized in Table 1. Intensity data were also corrected for absorption (ψ-scans). The structure of **1** was solved by standard Patterson and difference Fourier syntheses, whereas the structure of **2** was solved by direct methods using the SHELXS program (G. M. Sheldrick, Göttingen). The function minimized during least-squares refinements was $\Sigma w(|F_o| - |F_c|)^2$ with final convergence to $R = \Sigma ||F_o| - |F_c|| / \Sigma |F_o|$ and $R_w = [\Sigma w(|F_o| - |F_c|)^2 / \Sigma |F_o|^2]^{1/2}$ where $w = 1/\sigma^2(I)$. The positions of methyl and methylene H atoms were calculated (d(C–H) = 0.96 Å, sp^3-hybridized C atoms) and were included in the final refinement cycle with isotropic thermal parameters (see 'Supplementary Material'). All other non-hydrogen atoms were refined with anisotropic thermal parameters. During all calculations the analytical scattering factors for neutral atoms were corrected for both $\Delta f'$ and $i(\Delta f'')$ terms [14]. The final positional parameters for **1** are given in Table 2 those for **2** in Table 3. See 'Supplementary Material' for further details of the structure determinations.

Results and Discussion

The structure of the binuclear monocation in pale-greenish crystals of **1** is shown in Fig. 1; selected bond distances and angles are summarized in Table 4. Two high spin manganese(II) ions are bridged by a μ-hydroxo group and two symmetrical μ-acetato ligands. The pseudo-octahedral environment of both Mn atoms is completed by a facially coordinated cyclic amine ligand L. The overall structure is thus similar to a series of homo- and heterobinuclear complexes containing a variety of divalent first-row transition metals such as Fe(II), Co(II), Ni(II) [15]. The binuclear monocation in **1** possesses crystallographically imposed C_2 symmetry. The PF_6 anion

TABLE 1. Summary of crystallographic data

	1	2
Formula	$C_{23}H_{53}N_6F_6Mn_2O_6P$	$C_{16}H_{38}N_6I_4Mn_2O_6$
Formula weight	764.5	1028
Crystal system	tetragonal	monoclinic
Space group	$P4_12_1$	$P2_1/n$
a (Å)	11.04(1)	14.109(6)
b (Å)		21.096(6)
c (Å)	28.48(2)	21.007(7)
β (°)		97.05(4)
V (Å^3)	3471.2	6205.3
D_{calc} (g cm^{-1})	1.45	2.20
Crystal dimensions (mm)	0.23 × 0.34 × 0.65	0.3 × 0.25 × 0.35
Temperature (°C)	20	20
Radiation	Mo Kα (graphite)	Mo Kα (graphite)
Scan type	ϑ-2ϑ	ω
2ϑ range (°)	$3 < 2\vartheta < 60$	$3 < 2\vartheta < 56$
Data collected	$+h, +k, +l$	$+h, +k, +l$
No. data collected	2093	6773
No. unique data	1817 ($I > 2.5\sigma(I)$)	6175 ($I > 2.5\sigma(I)$)
Absorption coefficient (cm^{-1})	8.14	47.6
Transmission coefficients	0.9–1.0	0.81–1.0
Least-squares parameters	236	625
R	0.062	0.045
R_w	0.052	0.037
Goodness of fit	3.22	1.63

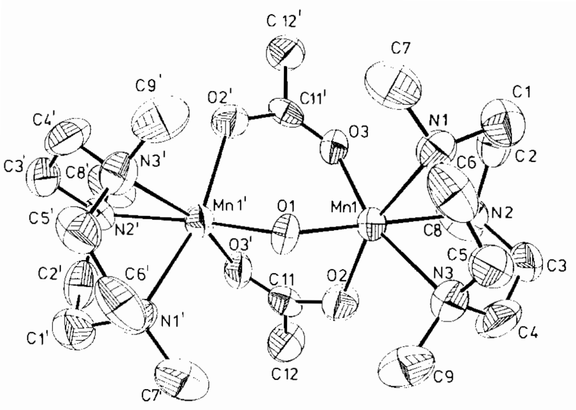

Fig. 1. The structure of the monocation in crystals of **1**.

TABLE 2. Atom coordinates (X10^4) and temperature factors (Å^2 X 10^3) for 1

Atom	*x*	*y*	*z*	*U*
Mn(1)	1637(1)	−124(1)	4663(1)	42(1)*
O(1)	1516(4)	1516(4)	5000	42(2)*
O(2)	1357(5)	−1206(5)	5303(2)	61(2)*
O(3)	−193(5)	−242(5)	4428(2)	56(2)*
C(11)	451(8)	−1036(8)	5569(3)	44(3)*
C(12)	272(9)	−2101(8)	5896(3)	74(4)*
N(1)	2341(7)	660(7)	3972(2)	58(3)*
N(2)	2051(6)	−1848(7)	4220(2)	51(3)*
N(3)	3747(6)	−312(7)	4715(3)	58(3)*
C(1)	2429(9)	−302(8)	3581(3)	78(5)*
C(2)	1765(9)	−1445(8)	3727(3)	71(4)*
C(3)	3330(9)	−2238(9)	4265(3)	68(4)*
C(4)	3948(9)	−1619(9)	4660(3)	79(4)*
C(5)	4353(8)	331(10)	4343(3)	70(5)*
C(6)	3507(10)	1226(10)	4111(3)	82(5)*
C(7)	1525(11)	1594(10)	3800(4)	92(6)*
C(8)	1227(10)	−2855(8)	4336(3)	82(5)*
C(9)	4136(9)	150(10)	5193(3)	83(5)*
P(1)	5550(3)	5550(3)	0	62(1)*
F(11)	6492(7)	4631(6)	156(2)	137(4)*
F(12)	4743(19)	5190(20)	403(8)	152(13)*
F(13)	5985(37)	6385(23)	365(8)	187(19)*
F(14)	4614(17)	4614(17)	0	256(19)*
F(15)	6482(20)	6482(20)	0	244(32)*
F(16)	5480(62)	5775(57)	543(10)	401(37)*
C(15)	2367(12)	2367(12)	0	126(6)*
C(16)	2473(16)	1491(17)	298(7)	71(9)*

Starred items: equivalent isotropic *U* defined as one third of the trace of the orthogonalised U_{ij} tensor.

TABLE 3. Atom coordinates (X10^4) and temperature factors (Å^2 X 10^3) for 2

Atom	*x*	*y*	*z*	*U*
I(1)	4219(1)	437(1)	2878(1)	56(1)*
I(2)	−52(1)	1474(1)	6144(1)	59(1)*
I(3)	4192(1)	527(1)	8112(1)	58(1)*
I(4)	3479(1)	1458(1)	8935(1)	48(1)*
I(5)	2688(1)	2487(1)	9717(1)	57(1)*
I(6)	4976(1)	3480(1)	6244(1)	56(1)*
I(7)	4343(1)	2426(1)	5245(1)	72(1)*
I(8)	3892(1)	1549(1)	4220(1)	79(1)*
Mn(1)	7742(1)	399(1)	3811(1)	30(1)*
Mn(2)	7544(1)	1409(1)	2734(1)	28(1)*
O(1)	7078(4)	1023(3)	3386(3)	31(2)*
O(2)	8146(4)	−111(3)	3054(3)	40(2)*
O(3)	8149(4)	648(3)	2308(3)	41(2)*
C(1)	8337(6)	93(4)	2521(4)	31(3)*
C(2)	8825(7)	−349(5)	2109(5)	47(4)*
O(4)	9026(4)	873(3)	3954(3)	37(2)*
O(5)	8842(4)	1660(3)	3231(3)	37(2)*
C(3)	9278(7)	1387(4)	3706(4)	38(4)*
C(4)	10166(7)	1688(5)	4045(5)	52(4)*
N(1)	6457(5)	−139(3)	3872(4)	39(3)*
N(2)	8319(5)	−344(3)	4373(3)	36(3)*
N(3)	7390(5)	691(4)	4758(4)	37(3)*
C(5)	6790(7)	−802(4)	3887(5)	50(4)*
C(6)	7637(7)	−888(4)	4392(5)	51(4)*
C(7)	8667(7)	−85(5)	5035(5)	48(4)*
C(8)	7877(7)	276(5)	5283(4)	44(4)*
C(9)	6348(6)	697(5)	4708(5)	49(4)*
C(10)	5953(7)	53(4)	4429(4)	41(4)*
N(4)	6214(5)	1306(3)	2098(3)	35(3)*
N(5)	7874(5)	1923(3)	1953(3)	37(3)*
N(6)	6838(5)	2318(3)	2885(3)	39(3)*
C(11)	6497(7)	1279(4)	1449(4)	44(4)*
C(12)	7170(7)	1831(5)	1376(4)	41(4)*
C(13)	7996(7)	2604(4)	2153(5)	46(4)*
C(14)	7109(7)	2828(4)	2438(5)	43(4)*
C(15)	5799(6)	2176(5)	2816(5)	44(4)*
C(16)	5513(7)	1823(4)	2180(5)	44(4)*
Mn(3)	7849(1)	356(1)	8850(1)	28(1)*
Mn(4)	7615(1)	1362(1)	7768(1)	30(1)*
O(6)	7140(4)	944(3)	8394(3)	32(2)*
O(7)	8351(5)	−116(3)	8115(3)	38(3)*
O(8)	8193(4)	609(3)	7341(3)	41(2)*
C(21)	8413(7)	61(5)	7550(5)	43(4)*
C(22)	8787(8)	−399(5)	7104(5)	52(4)*
O(9)	9117(4)	868(3)	9028(3)	37(2)*
O(10)	8912(5)	1613(3)	8262(3)	44(3)*
C(23)	9385(6)	1350(4)	8742(4)	33(3)*
C(24)	10359(6)	1612(5)	8974(5)	45(4)*
N(7)	6640(5)	−294(4)	8895(4)	43(3)*
N(8)	7334(5)	673(4)	9742(4)	36(3)*
N(9)	8495(5)	−319(3)	9485(3)	33(3)*
C(25)	6070(7)	−119(5)	9417(5)	52(4)*
C(26)	6289(7)	557(5)	9642(5)	48(4)*
C(27)	7854(7)	328(5)	10310(4)	40(4)*
C(28)	8743(7)	0(4)	10113(4)	42(4)*
C(29)	7897(7)	−902(4)	9517(4)	41(4)*
C(30)	7089(7)	−923(4)	8978(4)	48(4)*
N(10)	6284(5)	1298(4)	7114(4)	42(3)*
N(11)	6896(6)	2239(4)	7993(4)	44(3)*
N(12)	7960(6)	1933(4)	7032(4)	51(4)*

(continued)

TABLE 3. *(continued)*

Atom	*x*	*y*	*z*	*U*
C(31)	5602(7)	1794(4)	7237(5)	46(4)*
C(32)	5847(7)	2080(5)	7895(4)	49(4)*
C(33)	7196(9)	2776(5)	7606(5)	65(5)*
C(34)	8078(8)	2590(5)	7295(5)	64(5)*
C(35)	7236(8)	1893(6)	6438(5)	61(5)*
C(36)	6595(8)	1316(5)	6469(4)	65(5)*
W(1)	6913(7)	2096(4)	9580(4)	92(4)*
W(2)	5303(6)	2142(4)	254(4)	96(4)*

Starred items: equivalent isotropic *U* defined as one third of the trace of the orthogonalised U_{ij} tensor.

TABLE 4. Selected bond distances (Å) and angles (°) for 1

Mn1–O1	2.053(4)	Mn1–O2	2.200(6)
Mn1–O3	2.132(6)	Mn1–N1	2.286(7)
Mn1–N2	2.329(7)	Mn1–N3	2.343(7)
O3–C11′	1.205(10)	Mn1····Mn1′	3.351(3)
C11–C12	1.511(12)		
O1–Mn1–O2	94.8(2)	O1–Mn1–O3	98.0(2)
O2–Mn1–O3	95.4(2)	O1–Mn1–N1	95.2(2)
O2–Mn1–N1	165.0(3)	O3–Mn1–N1	94.3(2)
O1–Mn1–N2	170.6(2)	O2–Mn1–N2	91.8(2)
O3–Mn1–N2	88.0(2)	N1–Mn1–N2	77.1(2)
O1–Mn1–N3	96.5(2)	O2–Mn1–N3	92.3(2)
O3–Mn1–N3	163.0(2)	N1–Mn1–N3	75.5(3)
N2–Mn1–N3	76.5(2)	Mn1–O1–Mn1′	109.4(3)
Mn1–O2–C11	121.7(5)	Mn1–O3–C11′	133.8(6)
O2–C11–C12	110.8(7)	O2–C11–O3′	120.1(8)
C12–C11–O3′	121.0(8)		

displays some degree of disorder which is borne out by large anisotropic thermal parameters of the fluorine atoms; the interstitial methanol is also disordered.

The Mn–N and Mn–O distances are typical for octahedral high spin manganese(II). The average Mn–N bond length is 2.319 Å; the three Mn–N distances are within experimental error equivalent [16]. The Mn–O_{acetat} bond lengths are found at 2.200(6) and 2.132(6) Å whereas the Mn–$O_{hydroxo}$ bond is significantly shorter at 2.053(4) Å. The Mn^{II}–O distances of μ-alkoxo or μ-phenoxo bridges [17] are also longer ($\approx$2.13 Å). The Mn–O–Mn bond angle is 109.4(3)° and the Mn···Mn separation is 3.351(3) Å which is to be compared with the Mn···Mn distance at 3.6 Å in the catalase from *Thermus thermophilus* [1f]. The C–N and C–C bond lengths of the coordinated amine ligand are in the usual range observed for C–N and C–C single bonds. These ligands are not disordered as is frequently observed in crystal structures of binuclear species containing these ligands [15d]. Thus the present crystal structure determination of 1 gives reliable bond distances and angles. Due to steric constraints of the nine-membered macrocycle the N–Mn–N angles deviate by 13.6° from the octahedral angle of 90°.

The magnetic susceptibility of a powdered sample of $[L_2Mn_2(OH)(O_2CCH_3)_2](ClO_4)$ has been measured in the temperature range 90–300 K by using the Faraday method. The magnetic moment of the complex was found to decrease with decreasing temperature (Fig. 2). The data were readily analyzed by using the Heisenberg, Dirac, van Velck isotropic exchange model [18], $\mathcal{H} = -2J\hat{S}_1\cdot\hat{S}_2$ with $S_1 = S_2 = 5/2$. The solid curve in Fig. 2 represents a least-squares fit of the data to the above equation by using parameters $J = -9(1)$ cm^{-1} and $g = 1.98(2)$. This behavior indicates intramolecular antiferromagnetic spin exchange coupling of the two high spin manganese(II) ions in the monocation of **1**. The magnitude of this antiferromagnetic coupling is significantly larger than in analogous binuclear species containing μ-alkoxo or μ-phenoxo bridges [17]. It indicates that μ-hydroxo bridges are better mediators for a superexchange mechanism than either of the above mentioned alkoxo or phenoxo groups. In the corresponding tris-μ-acetato–dimanganese(II) complex $[L_2Mn_2(\mu\text{-}CH_3CO_2)_3]^+$, the *J* value is only -1.7 cm^{-1} [9]. Interestingly, it is observed that the two high spin ferrous ions in the corresponding complex $[L_2Fe_2(\mu\text{-}OH)(\mu\text{-}CH_3CO_2)_2]^+$ are also antiferromagnetically coupled. The observed *J* value of -13 cm^{-1} is of the same order of magnitude as in **1** [15d].

Finally, it is noted that the Mn–O distance of a bridging water molecule between two high spin Mn(II) ions is significantly longer (av. 2.353 Å) [19] than the present Mn–$O_{hydroxo}$ bond lengths. It is therefore anticipated that the intramolecular exchange coupling in a μ-aqua-bis(μ-acetato)dimanganese(II) core is significantly smaller than in 1.

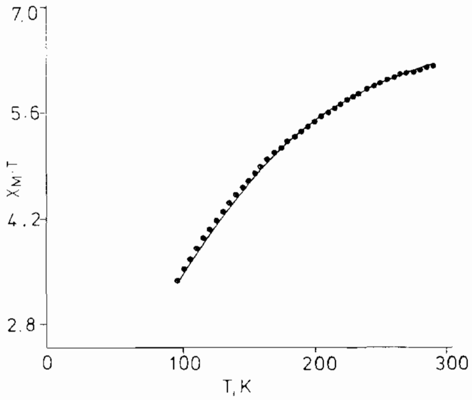

Fig. 2. Plot of $\chi_M T$ vs. *T* for $[L_2Mn_2(OH)(O_2CCH_3)_2]$-$(ClO_4)$.

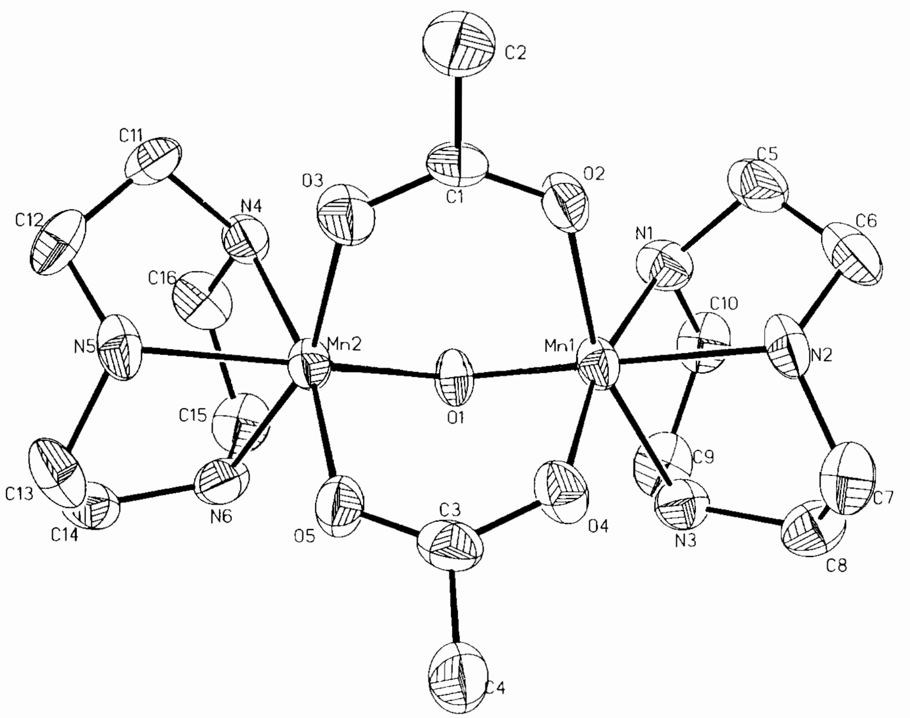

Fig. 3. The structure of one crystallographically independent dication in crystals of 2.

Crystals of 2 consist of the binuclear dication $[L'_2Mn_2(O)(CH_3CO_2)_2]^{2+}$ uncoordinated iodide, $(I_3)^-$ anions and water molecules of crystallization. There are two crystallographically independent sites for the dications per unit cell. Figure 3 displays the structure of one crystallographically independent dication in black–red crystals of 2; selected bond distances and angles are summarized in Table 5.

TABLE 5. Selected bond distances (Å) and angles (°) for 2 (values for one dication are given only)

I3–I4	2.879(1)	I4–I5	3.017(1)
I6–I7	3.112(1)	I7–I8	2.851(1)
Mn1···Mn2	3.096(2)	Mn1–O1	1.790(6)
Mn1–O2	2.057(6)	Mn1–O4	2.059(6)
Mn1–N1	2.156(8)	Mn1–N2	2.069(7)
Mn1–N3	2.199(8)	Mn2–O1	1.787(6)
Mn2–O3	2.072(6)	Mn2–O5	2.063(6)
Mn2–N4	2.176(7)	Mn2–N5	2.066(8)
Mn2–N6	2.200(7)	O2–C1	1.258(11)
O3–C1	1.271(10)	C1–C2	1.496(14)
O4–C3	1.273(11)	O5–C3	1.246(11)
C3–C4	1.503(13)		
I3–I4–I5	176.1(1)	I6–I7–I8	172.7(1)
O1–Mn1–O2	100.2(2)	O2–Mn1–O4	92.5(3)
O1–Mn1–O4	96.5(3)	O1–Mn1–N1	91.4(3)
O2–Mn1–N1	94.9(3)	O4–Mn1–N1	168.0(3)
O2–Mn1–N2	85.4(3)	O1–Mn1–N2	170.9(3)
N1–Mn1–N2	80.9(3)	O4–Mn1–N2	90.4(3)
O1–Mn1–N3	94.7(3)	O2–Mn1–N3	164.0(3)
O4–Mn1–N3	91.4(3)	N1–Mn1–N3	78.9(3)
N2–Mn1–N3	79.1(3)	O1–Mn2–O3	100.8(3)
O3–Mn2–O5	91.7(2)	O1–Mn2–O5	96.6(2)
O1–Mn2–N4	93.1(3)	O3–Mn2–N4	91.5(3)
O5–Mn2–N4	169.0(3)	O3–Mn2–N5	85.3(3)
O1–Mn2–N5	171.0(3)	N4–Mn2–N5	80.0(3)
O5–Mn2–N5	89.7(3)	O1–Mn2–N6	94.0(3)
O3–Mn2–N6	162.7(3)	O5–Mn2–N6	95.4(2)
N4–Mn2–N6	78.7(3)	N5–Mn2–N6	79.0(3)
Mn1–O1–Mn2	119.9(3)	Mn1–O2–C1	128.2(5)
Mn2–O3–C1	129.9(6)	O2–C1–O3	124.7(8)
O2–C1–C2	117.8(8)	O3–C1–C2	117.5(8)
Mn1–O4–C3	129.7(6)	Mn2–O5–C3	127.4(6)
O4–C3–O5	125.8(8)	O4–C3–C4	115.1(8)
O5–C3–C4	119.0(8)		

The overall structure of the binuclear cation is identical with the structure determination of $[L'_2Mn_2(\mu\text{-}O)(CH_3CO_2)_2](ClO_4)_2$ [5] but in contrast to the previous analysis the present data are much more reliable, because the iodide and $(I_3)^-$ anions and water molecules of crystallization in 2 are ordered.

There are now three structure determinations of high quality reported of complexes containing the μ-oxo-bis(μ-acetato)dimanganese(III) core where the remaining coordination sites of the Mn(III)

TABLE 6. Comparison of structural data of complexes containing the μ-oxo-bis(μ-acetato)dimetal(III) core

Complex[a]	$M-O_{oxo}$ (Å)	$M-N_{trans}$ (Å)	$M-N_{cis}$ (Å)	$M-O_{acetato}$ (Å)	M–O–M (°)	M···M (Å)	Reference
2	1.788(6)	2.068(8)	2.166(8) 2.200(8)	2.062(6)	119.9(3)	3.096(2)	this work
3	1.780(2)	2.057(2)	2.173(3) 2.175(2)	2.068(2) 2.064(3)	125.1(1)	3.159(1)	7
4	1.783(5)	2.062(6)	2.054(6)	1.938(5)	122.9		6
5	1.781(4)	2.205(7)	2.165(6)	2.042(6)	118.7(3)	3.063(2)	20
6	1.792(4)	2.228(5)	2.158(6)	2.048(8)	130.2(2)	3.250(2)	21

[a] 3, $[Mn_2O(O_2CCH_3)_2(HB(pz)_3)_2]\cdot 4CH_3CN$; 4, $[Mn_2O(O_2CCH_3)_2(H_2O)_2(bipy)_2](PF_6)_2\cdot(H_2O)_{1.75}$; 5, $[L'_2Fe_2O(O_2CCH_3)_2]I_2\cdot 0.5CH_3CN$; 6, $[L_2V_2O(O_2CCH_3)_2]I_2\cdot 2H_2O$.

centers are occupied by either tridentate ligands (trispyrazolylborate [7], 1,4,7-triazacyclononane, *N,N',N"*-trimethyl-1,4,7-triazacyclononane [5]) or 2,2-bipyridine and one water molecule [6]. The salient feature of this core in comparison with the corresponding diiron(III) [20] and divanadium(III) [21] species is the apparent lack of a pronounced structural *trans* influence of the $Mn-O_{oxo}$ bond on the *trans* Mn–N bond distances. In fact these distances are *shorter* than the *cis* Mn–N bond distances. In the diiron(III) and divanadium(III) complexes (Table 6) the structural *trans* influence is clearly detected. The difference $[(M-N_{trans})-(M-N_{cis})]$ is 0.04 Å for the diiron(III) and 0.07 Å for the divanadium(III) complex.

For the dimanganese(III) complexes the shortening of the Mn–N bond with respect to the $Mn-N_{cis}$ bonds has been interpreted by Sheats *et al.* [7] as follows: 'The short $Mn-O_{oxo}$ bond raises the energy of the d_{z^2} orbital directed along the $Mn-O_{oxo}$ bond vector. This highest lying d orbital is empty in high spin, d^4 Mn(III), resulting in a shortened *trans* Mn–N bond. In high spin iron(III), the corresponding d_{z^2} orbital is occupied, and the Fe–N bond is lengthened.' This model does not account correctly for the observation that the divanadium(III) complex (d^2) shows the most pronounced *trans* influence despite the fact that both the d_{z^2} and $d_{x^2-y^2}$ orbitals are empty. Therefore, we suggest a Jahn–Teller distortion of the high spin d^4 Mn(III) ion along the $Mn-O_{oxo}$ bond vector (*z* axis). A compressed octahedron would then require a short $Mn-O_{oxo}$ *and* a short $Mn-N_{trans}$ bond distance whereas the remaining $Mn-N_{cis}$ and $Mn-O_{acetate}$ bond distances are somewhat elongated. This is nicely borne out by the observation that the $Mn-N_{cis}$ bonds in the dimanganese(III) complex 2 are as long or even longer than the $Fe-N_{cis}$ distances in $[L'_2Fe_2O(O_2CCH_3)_2]^{2+}$ [20] although the ionic radii of both transition metal ions are identical. The structural *trans* influence of the oxo group is primarily due to its π-donating capability which repels the ligand in the *trans* position no matter if the d_{z^2} orbitals are occupied or not. Thus in the case of the dimanganese(III) complex a Jahn–Teller compressed octahedral geometry predicts a short $Mn-N_{trans}$ bond which is internally still somewhat elongated by the *trans* oxo π-donator. Noteworthy in this respect is the observation that in Girerd's dimanganese(III) complex $[Mn_2O(O_2CCH_3)_2(H_2O)_2(bipy)_2](PF_6)_2(H_2O)_{1.75}$ the $Mn-N_{trans}$ and $Mn-N_{cis}$ bond lengths are identical within experimental error.

Supplementary Material

Further details of the crystal structure investigations may be obtained from the Fachinformationszentrum Energie, Physik, Mathematik GmbH, D-7514 Eggenstein-Leopoldshafen 2, F.R.G. on quoting the depository number CSD 53839, the names of the authors, and the journal citation.

Acknowledgements

We thank the Deutsche Forschungsgemeinschaft and the Fonds der Chemischen Industrie for financial support of this work.

References

1 (a) V. V. Barynin and A. I. Grebenko, *Dokl. Akad. Nauk, SSR, 288* (1986) 1100; (b) V. V. Barynin, A. A. Vagin, V. R. Melik-Adamyan, A. I. Grebenko, S. V. Khangulov, A. N. Popov, M. W. Andrianova and B. K. Vainshtein, *Dokl. Akad. Nauk, SSR, 288* (1986) 877; (c) B. K. Vainshtein, V. R. Melik-Adamyan and V. V. Barynin, *Kristallografia, 26* (1981) 10003; (d) S. V. Khangulov, V. V. Barynin, V. R. Melik-Adamyan, A. I. Grebenko, N. V. Voevodskaya, L. A. Blumenfeld, S. N. Dobryakov and U. B. Ilyasova, *Bioorg. Khim., 12* (1986) 741; (e) S. V. Khangulov, N. V. Voevodskaya, V. V. Barynin, A. I. Grebenko and V. R. Melik-Adamyan, *Biofizika, 32* (1987) 960; (f) B. K. Vainshtein, W. R.

Melik-Adamyan, V. V. Barynin, A. A. Vagin and A. I. Grebenko, *Proc. Int. Symp. Biomol. Struct. Interactions, Suppl. J. Biosci.*, *8* (1985) 471.

2 (a) Y. Kono and I. Fridovich, *J. Biol. Chem.*, *258* (1983) 6015; (b) W. F. Beyer, Jr. and I. Fridovich, *Biochemistry*, *24* (1985) 6460.

3 R. M. Franko and J. E. Penner-Hahn, *J. Am. Chem. Soc.*, *110* (1988) 7554.

4 (a) A. Willing, H. Follmann and G. Auling, *Eur. J. Biochem.*, *170* (1988) 603; (b) J. Plönzig and G. Auling, *Arch. Microbiol.*, *146* (1987) 396.

5 K. Wieghardt, U. Bossek, D. Ventur and J. Weiss, *J. Chem. Soc., Chem. Commun.*, (1985) 347.

6 S. Ménage, J. J. Girerd and A. Gleizes, *J. Chem. Soc., Chem. Commun.*, (1988) 431.

7 J. E. Sheats, R. S. Czernuszewicz, G. C. Dismukes, A. L. Rheingold, V. Petrouleas, J. Stubbe, W. H. Armstrong, R. H. Beer and S. J. Lippard, *J. Am. Chem. Soc.*, *109* (1987) 1435.

8 Y. Nishida, N. Oshino and T. Tokii, *Z. Naturforsch., Teil B*, *43* (1988) 637.

9 K. Wieghardt, U. Bossek, B. Nuber, J. Weiss, J. Bonvoisin, M. Corbella, S. E. Vitols and J. J. Girerd, *J. Am. Chem. Soc.*, *110* (1988) 7398.

10 K. Wieghardt, U. Bossek, J. Bonvoisin, P. Beauvillain, J. J. Girerd, B. Nuber, J. Weiss and J. Heinze, *Angew. Chem.*, *98* (1986) 1026; *Angew. Chem. Int. Ed. Engl.*, *25* (1986) 1030.

11 (a) M. Suzuki, S. Murata, A. Uehara and S. Kida, *Chem. Lett.*, (1987) 281; (b) M. Suzuki, M. Mikuriya, S. Murata, A. Uehara, H. Oshio, S. Kida and K. Saito, *Bull. Chem. Soc. Jpn.*, *60* (1987) 4305; (c) H. Diril, H.-R. Chang, X. Zhang, S. K. Larsen, J. A. Potenza, C. G. Pierpont, H. J. Schugar, S. S. Isied and D. N. Hendrickson, *J. Am. Chem. Soc.*, *109* (1987) 6207; (d) R. M. Buchanan, K. J. Oberhausen and J. F. Richardson, *Inorg. Chem.*, *27* (1988) 971; (e) H. R. Chang, H. Diril, M. J. Nilges, X. Zhang, J. A. Potenza, H.-J. Schugar, D. N. Hendrickson and S. S. Isied, *J. Am. Chem. Soc.*, *110* (1988) 625.

12 T. J. Atkins, J. E. Richman and W. F. Oettle, *Org. Synth.*, *58* (1978) 86.

13 K. Wieghardt, P. Chaudhuri, B. Nuber and J. Weiss, *Inorg. Chem.*, *21* (1982) 3086.

14 *International Tables for X-ray Crystallography*, Vol. IV, Kynoch Press, Birmingham, U.K., 1974.

15 (a) P. Chaudhuri, M. Winter, H.-J. Küppers, K. Wieghardt, B. Nuber and J. Weiss, *Inorg. Chem.*, *26* (1987) 3302; (b) P. Chaudhuri, H.-J. Küppers, K. Wieghardt, S. Gehring, W. Haase, B. Nuber and J. Weiss, *J. Chem. Soc., Dalton Trans.*, (1988) 1367; (c) P. Chaudhuri, J. Querbach, K. Wieghardt, B. Nuber and J. Weiss, *J. Chem. Soc., Dalton Trans.*, in press; (d) J. R. Hartman, R. L. Rardin, P. Chaudhuri, K. Pohl, K. Wieghardt, B. Nuber, J. Weiss, G. C. Papaefthymiou, R. B. Frankel and S. J. Lippard, *J. Am. Chem. Soc.*, *109* (1987) 7387.

16 K. Wieghardt, U. Bossek, B. Nuber and J. Weiss, *Inorg. Chim. Acta*, *126* (1987) 39.

17 D. P. Kessissoglou, W. M. Butler and V. L. Pecoraro, *Inorg. Chem.*, *26* (1987) 495.

18 C. J. O'Connor, *Prog. Inorg. Chem.*, *29* (1982) 203.

19 M. Rüegg, A. Ludi and K. Rieder, *Inorg. Chem.*, *10* (1973) 1773.

20 (a) K. Wieghardt, K. Pohl and W. Gebert, *Angew. Chem., Int. Ed. Engl.*, *22* (1983) 727; (b) A. Spool, I. D. Williams and S. J. Lippard, *Inorg. Chem.*, *24* (1985) 2156.

21 M. Köppen, G. Fresen, K. Wieghardt, R. M. Llusar, B. Nuber and J. Weiss, *Inorg. Chem.*, *27* (1988) 721.